An experimental study of a base-isolation system using laminated rubber bearings and viscous dampers

M.Higashino, S.Aizawa & Y.Hayamizu
Takenaka Komuten Co. Ltd, Tokyo, Japan

ABSTRACT

The authors have performed tests on their earlier developed base-isolation system, which uses laminated rubber bearings and viscous dampers. In 1984, we constructed a full-scale model (supporting 505 ton of weight), and, using this system, carried out a free vibration test. Twelve seismometers were installed in this structure, enabling us to observe its earthquake response.

From the free vibration test, earthquake records, and a simulation analysis, we confirmed the effectiveness of the base-isolation system.

1 INTRODUCTION

Recently, the base-isolation system has been widely studied, and many kinds of systems have been developed. Presently, base-isolation systems using laminated rubber bearings are considered to be one of the most practical methods of reducing the acceleration response of buildings during earthquakes; and the system has been adopted for use in several countries. Especially in Japan, many kinds of systems have been developed in the past 2 or 3 years, but most of these systems use the histerisis of steel as an energy-absorbing device.

The authors started experimental study on the base-isolation system in 1982. Here the viscous damper, using the shear deformation of viscous fluid, is employed as an energy-absorbing device. The viscous damper does not have noticeable initial stiffness, as do steel dampers. This fact leads to the following characteristics: 1) the movement of the structure during an earthquake is smooth; 2) the viscous damper does not raise the natural frequency of the system; 3) the damping ratio can be set independently from the natural frequency of the system, [in other words, it is easy to design the system]; and 4) base-isolation is effective for earthquakes whether large or small.

Having these characteristics, this system is suitable not only for buildings of regular use but also for high value-added buildings, such as precision environmental facilities, hospitals, etc., which can tolerate neither large nor small earthquakes.

The authors constructed a full-scale model, supporting 505 ton of weight with laminated rubber bearings and viscous dampers. We have carried out free vibration tests of this model and have been

also observing its behavior during earthquakes. The results of these studies are shown below.

2 VISCOUS DAMPER

The viscous damper has the mechanism shown in Fig.1. The damping force is provided by the shear deformation of the viscous fluid between the upper plate and the base plate. Fig. 2 shows the forced vibration test results of the damper itself (upper plate area A=908 cm^2). The figure shows the relationship between shear velocity (velocity divided by the thickness of the viscous fluid) and resistance force. From this test, the characteristics of this damper are expressed in the following formula:

$$F=0.42 \times e^{-0.043T} \times A \times (v/d)^{0.59} \qquad (1)$$

where F is the damping force (kg), T the temperature (°C), A the upper plate area (m^2), v the velocity of the upper plate to the base plate (cm/sec), and d the thickness of the fluid (cm).

3 THE MODEL AND FREE VIBRATION TEST

The model was built at the Takenaka Technical Laboratory site in Tokyo. The superstructure of the model was used for two other studies: "Variable Section Slip-Form Process Test," and "Coal-Storing Silo Test." It is 11.5 meters in height, 9 meters in diameter at the bottom, and its weight is 505 ton. This structure is supported by 9 laminated bearings. 6 viscous dampers are set beneath the superstructure.

The laminated rubber bearings are designed to make the natural frequency of the structure 0.5 Hz when they support 50 ton each. Each bearing is composed of 30 pieces of natural-rubber sheets (0.5 cm thick) and 29 pieces of steel plate (0.3 cm thick). The stiffness of one rubber bearing is 547 kg/cm in the horizontal direction and 6.07×10^5 kg/cm in the vertical direction (Fig. 4).

Fig. 5 shows the shape of the viscous damper. In this damper, the area of the upper plate is 755 cm^2, and the thickness of the viscous fluid is 0.6 cm. The damper is designed to show 10% damping ratio at 20 cm/sec velocity movement at 20°C temperature.

In the free vibration test, a notched steel rod (32ϕ) was attached to the superstructure. The free vibration was induced by pulling this rod with a center-holed jack until the rod was cut off. Fig. 6 shows the time histories of the free vibration. The broken line indicates the free vibration wave without viscous dampers, and the solid line indicates the free vibration with viscous dampers. From the test results, we can see that without the dampers the damping ratio is h_R=2.4%. We can see that the viscous damper is absorbing the vibration energy effectively. The observed damping ratio of free vibration with dampers is almost 12%.

Fig. 7 shows the relation between the natural period of the system and vibration amplitude. The natural period of the system is designed to be 2 seconds. But from the figure, we see that the period of the system becomes shorter in small-amplitude vibration when the viscous dampers are employed. The elasticity of the visco-elastic fluid was outstanding for small-amplitude vibration, but the variation of the

resonance frequency was small. As mentioned above, the damping ratio of the system is related to the velocity of the superstructure. The relation between these two is shown in Fig. 8. The results from the free vibration test (shown in dots) are distributed near the line calculated from formula (1). From this data, we can see that the system performed as designed.

4 BEHAVIOR DURING EARTHQUAKES

In the model, 12 seismometers (6 for horizontal and 6 for vertical) were installed to observe the acceleration response of the structure. In several earthquakes observed here, the one observed on October 4, 1985, was fairly large. Here we show the response of the model under this earthquake. Fig. 9 shows the acceleration record at the base of the model (below the system) and at the superstructure (above the system). From these records, it is known that the maximum acceleration levels were reduced by 0.63 and 0.37 for NS and EW directions, respectively. The difference between these two ratios was caused by the difference in input direction (Fig. 10). As the NS direction wave had spectrum peaks much closer to the structure's natural frequency than did the EW direction wave, the system did not reduce the NS direction acceleration as well as it reduced that of the EW direction.

In time histories and spectra, the response included higher frequency components; yet the natural frequency of the system is 0.5 Hz. This phenomenon is seen in the horizontal transfer function obtained from dividing the response spectrum by the input spectrum. In other words, the transfer function has many peaks that are higher than natural frequency. The rocking spectra at the base of the structure have peaks that are between 0 Hz and 10 Hz (Fig. 10). As the structure is tall in proportion, we can consider the higher frequency components to have been caused mainly by rocking vibration input.

A fairly large displacement occurred during this earthquake, and the displacement orbits are shown in Fig. 13. The recorded displacement orbit and the orbit obtained by integrating the acceleration record agree well.

5 THE SIMULATION ANALYSIS

The superstructure of the model is considered almost rigid. In the simulation analysis, the equation of motion is formulated in 1 mass 6 degrees of freedom system.

$$[M]\{\ddot{u}\}+\{F_D\}+[K]\{u\} = -[M]\{\ddot{g}\} \qquad (2)$$

where

$[M]$ is the Mass matrix
$\{u\} = \{X, Y, Z, \theta x, \theta y, \theta z\}^T$ <displacement vector>
$\{\ddot{g}\} = \{\ddot{X}g, \ddot{Y}g, \ddot{Z}g, \ddot{\theta}xg, \ddot{\theta}yg, \ddot{\theta}zg\}^T$ <input acceleration vector>

F_D is the sum of the damping force of the viscous dampers, given by formula (1), and the damping of the rubber bearings. In composing the stiffness matrix [K], the visco-elasticity of the damper is taken into account when the displacement is small.

The input acceleration is composed by transforming

5 observed acceleration records (2 horizontal, and 3 vertical) at the base of the model to global coordinate. The illustration shown in Fig. 11 describes the analyzing procedure. The stiffness and damping matrices are updated at every step of analysis.

In Fig. 12, the analyzed response acceleration is shown in comparison with the recorded wave (the October 4, 1985 earthquake). The analyzed wave shows good agreement with the recorded wave. Also the calculated displacement orbit shown in Fig. 13 agrees well with the other two orbits (the recorded orbit and the orbit obtained by integrating the acceleration record). We can see that the clearness of the characteristics of the devices and the simplicity of the vibration model make this so.

The accumulated damping energy is calculated by the following formula:

$$E_D = \int \{\dot{u}\} \cdot \{F_D\} dt \tag{3}$$

where

$$\{F_D\} = \{Fx, Fy\}^T \quad \text{<damping force vector>} \tag{4-a}$$

$$\{\dot{u}\} = \{\dot{X}, \dot{Y}\} \quad \text{<velocity vector>} \tag{4-b}$$

Assuming the behavior of the structure as 1 mass 6 degrees of freedom, the damping forces are obtained as follows.

$$_RFx = -M\ddot{Y} - M_I\ddot{\Theta}y - KY \tag{5-a}$$

$$_RFy = -M\ddot{X} - M_I\ddot{\Theta}x - KX \tag{5-b}$$

where M is the mass of the superstructure; M_I the inertia effecting the horizontal vibration; $\ddot{X}$, $\ddot{Y}$, $\ddot{\Theta}x$, $\ddot{\Theta}y$ the recorded acceleration at the diaphragm of the superstructure; K the horizontal stiffness read from transfer function; X, Y the related displacement obtained by integrating the acceleration record.

In Fig. 14, the accumulated damping energy time histories are shown. The "non-linear analysis" shown in the figure indicates the analyzed result using formula (1). The analysis also agrees with the energy record.

The equivalent damping factor is given by the following formula:

$$C_E = \frac{\int F_D \cdot \dot{u} dt}{\int \dot{u}^2 dt} \tag{6}$$

where F_D is the damping force.

The calculated accumulated energy using C_E is also shown in Fig. 14. The time history closely agrees with the history obtained by using nonlinear C. In Fig. 15, the calculated velocity using C_E is shown in comparison with the velocity, which is obtained by integrating the acceleration record. As seen in the figure, the linear analysis is very accurate.

6 CONCLUSIONS

1) From the free vibration test, it is confirmed that the viscous damper has good damping ability. Also, the laminated rubber bearing has good deformation ability, and its movement is very smooth.

2) From earthquake observations, the system worked well. However, its effectiveness depended on the characteristics of the earthquakes. In designing the base-isolated structure, it is necessary to know the ground's vibration characteristics as well as possible.

3) The results of the simulation analysis agreed closely with observation records. Consequently, the response characteristics of the structure can be estimated very accurately at the designing stage.

4) The analysis using equivalent damping coefficient C_E gives good results. Consequently, linearizing the analyzing procedure is valuable to the design of structures.

Based on these studies, we are constructing a building (supporting 2,400 ton). It will be completed in March 1987.

7 ACKNOWLEDGEMENTS

The laminated rubber bearings used in this study are the products of the Bridgestone Corporation, and the viscous dampers are the products of Oiles, Inc. The authors would like to thank these two companies for the support they gave to our studies.

8 REFERENCES

Jolivet F., et al. 1977. A Seismic Foundation System for Nuclear Power Stations. Proceedings of the 4th SMIRT.

Kelly, J.M., et al. Experimental Study of Lead and Elastomeric Dampers for Base Isolation Systems. USC/EERC - 81/16.

Hayamizu, Y., et al. A Study of an Earthquake Base-Isolation System Using Laminated Rubber Bearings. AIJ Annual Meeting, 1984-86.

Fujita, T., et al. An Aseismic Base-Isolation System Using Laminated Rubber Bearings for Heavy Mechnical Equipment (4th Report). SEISAN-KENKYU, University of Tokyo, Vol. 35, No. 4.

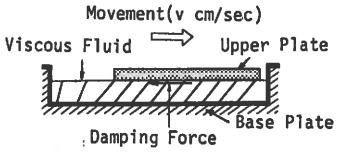

Fig.1 The Mechanism of Damping

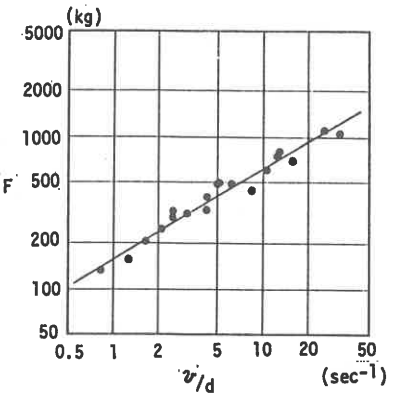

Fig.2 The Relation between Damping Force and Shear Velocity

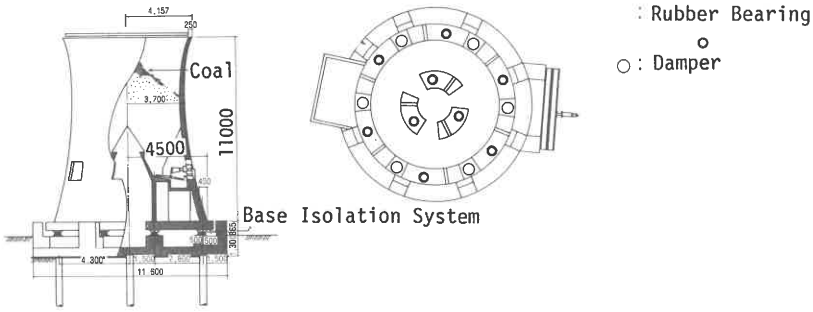

Fig.3 The Full Scale Model

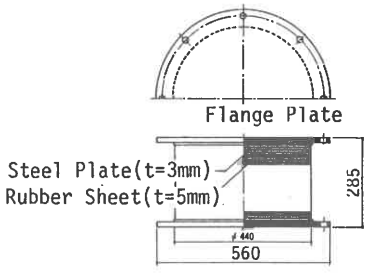

Fig.4 The Rubber Bearing

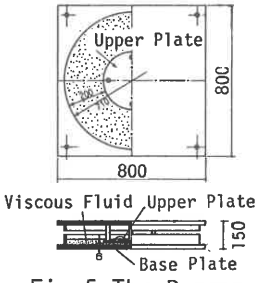

Fig.5 The Damper

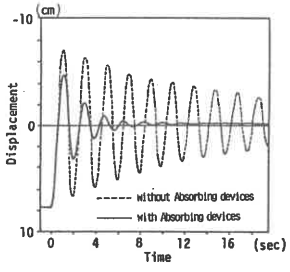

Fig.6 The Free Vibretion Time Histories

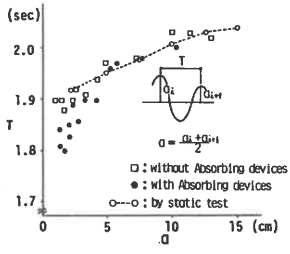

Fig.7 The Relation between Amplitude and Natural Period

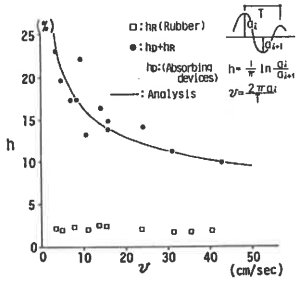

Fig.8 The Relation between Velocity and Damping Ratio

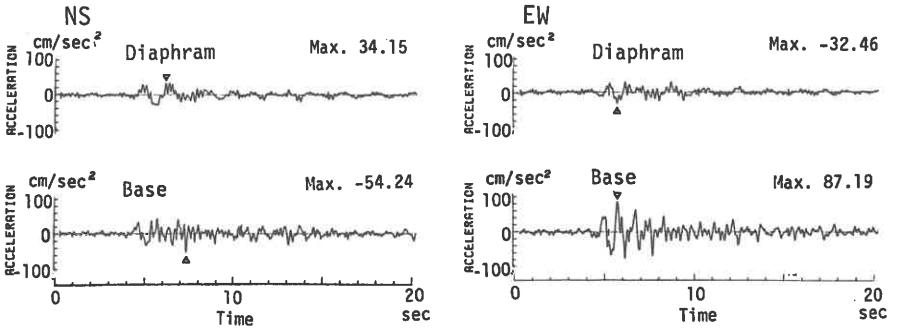

Fig.9 The Recorded Acceleration Time Histories of the Model
(Oct. 4 , 1985)

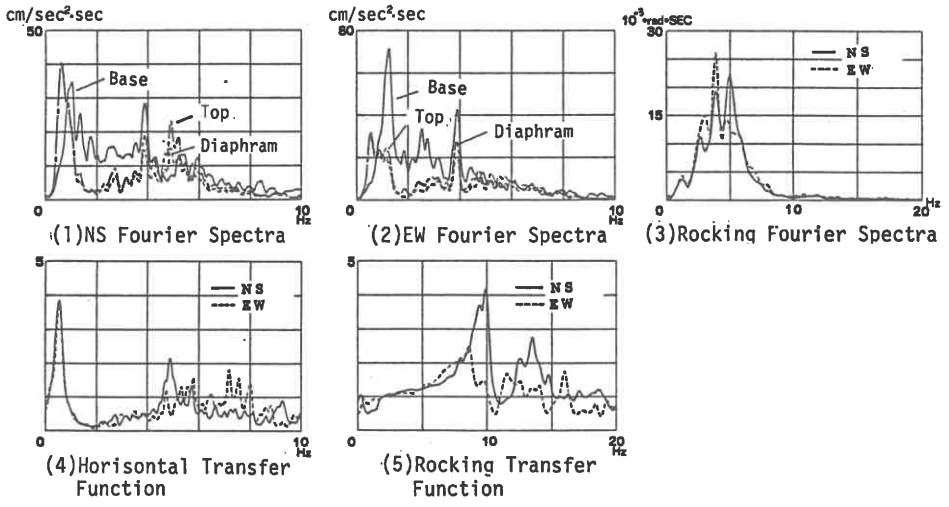

Fig.10 The Recorded Earthquake Acceleration Spectra (Oct.4.1985)

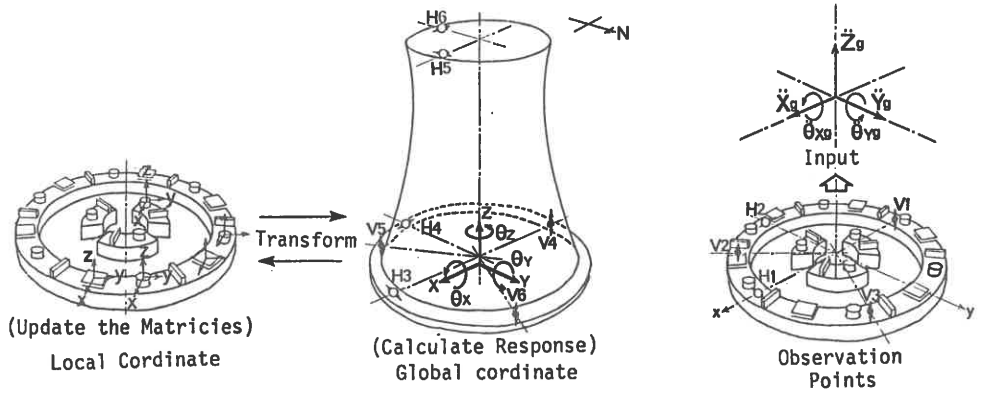

Fig.11 The Analyzing Procedure

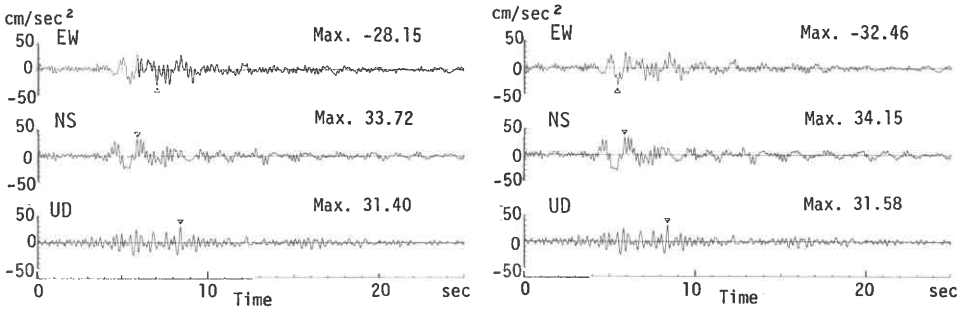

(1) Caluculated Response (2) Recorded Response

Fig.12 The Comparison of Acceleration Responses(Oct.4.1985)

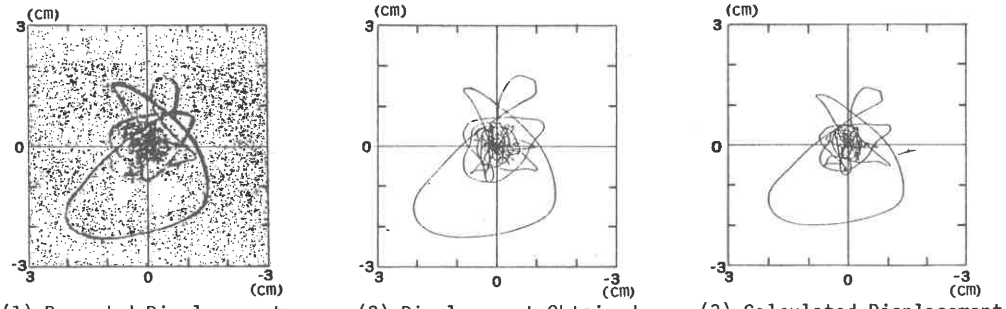

(1) Recorded Displacement (2) Displacement Obtained by Integrating Acceleration Record (3) Calculated Displacement

Fig.13 The Displacement Orbits

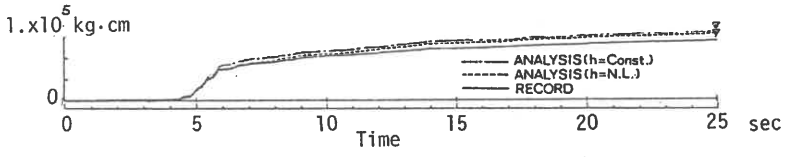

Fig.14 The Comparison of Accumulated Damping Energy

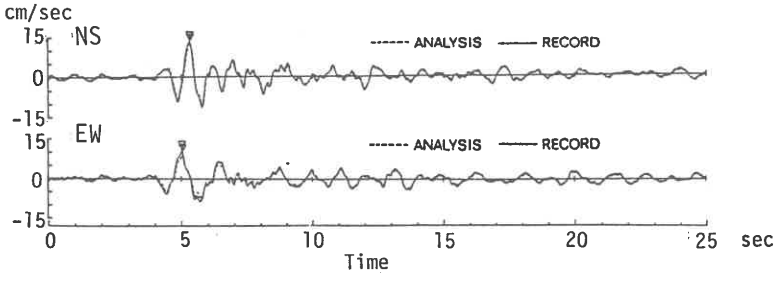

Fig.15 The Comparison of Response Velocity